

Relativistic Jets from Accretion Disks

R.V.E. Lovelace, P.R. Gandhi, & M.M. Romanova
Cornell University

October 5, 2018

Abstract

The jets observed to emanate from many compact accreting objects may arise from the twisting of a magnetic field threading a differentially rotating accretion disk which acts to magnetically extract angular momentum and energy from the disk. Two main regimes have been discussed, hydromagnetic jets, which have a significant mass flux and have energy and angular momentum carried by both matter and electromagnetic field and, Poynting jets, where the mass flux is small and energy and angular momentum are carried predominantly by the electromagnetic field. Here, we describe recent theoretical work on the formation of relativistic Poynting jets from magnetized accretion disks. Further, we describe new relativistic, fully-electromagnetic, particle-in-cell simulations of the formation of jets from accretion disks. Analog Z-pinch experiments may help to understand the origin of astrophysical jets.

1. INTRODUCTION

Powerful, highly-collimated, oppositely directed jets are observed in active galaxies and quasars (see for example Bridle & Eilek 1984), and in old compact stars in binaries - the “microquasars” (Mirabel & Rodriguez 1994; Eikenberry *et al.* 1998). Further, highly collimated emission line jets are seen in young stellar objects (Bührke, Mundt, & Ray 1988). Different models have been put forward to explain astrophysical jets (Bisnovatyi-Kogan & Lovelace 2001). Recent observational and theoretical work favors models where twisting of an ordered magnetic field threading an accretion disk acts to magnetically accelerate the jets. Here, we discuss the origin of the relativistic jets observed in active galaxies and quasars and in microquasars. We first discuss a theoretical model (§1), and then new results from relativistic particle-in-cell (PIC) simulations (§2).

2. POYNTING JETS

The powerful jets observed from active galaxies and quasars are probably not hydromagnetic outflows but rather Poynting flux dominated jets. The motions of these jets measured by very long baseline interferometry correspond to

bulk Lorentz factors of $\Gamma = \mathcal{O}(10)$ which is much larger than the Lorentz factor of the Keplerian disk velocity predicted for hydromagnetic outflows. Furthermore, the low Faraday rotation measures observed for these jets at distances < 1 kpc from the central object implies a very low plasma densities. Similar arguments indicate that the jets of microquasars are not hydromagnetic outflows but rather Poynting jets. Poynting jets have also been proposed to be the driving mechanism for gamma ray burst sources (Katz 1997). Theoretical studies have developed models for Poynting jets from accretion disks (Lovelace, Wang, & Sulkanen 1987; Lynden-Bell 1996; Romanova & Lovelace 1997; Levinson 1998; Li *et al.* 2001; Lovelace *et al.* 2002; and Lovelace & Romanova 2003). Stationary non-relativistic Poynting flux dominated outflows were found by Romanova *et al.* (1998) and Ustyugova *et al.* (2000) in axisymmetric MHD simulations of the opening of magnetic loops threading a Keplerian disk. Here, we summarize a model for the formation of relativistic Poynting jets from a disk (Lovelace & Romanova 2003).

Consider a dipole-like coronal magnetic field - such as that shown in the lower part of Figure 1a - threading a differentially rotating Keplerian accretion disk. The disk is perfectly conducting, high-density, and has a small accretion speed (\ll Keplerian speed). The field may be generated in the disk by a dynamo action and released. Outside of the disk there is assumed to be a ‘‘coronal’’ or ‘‘force-free’’ plasma ($\rho_e \mathbf{E} + \mathbf{J} \times \mathbf{B}/c \approx 0$, Gold & Hoyle 1960). We use cylindrical (r, ϕ, z) coordinates and consider axisymmetric field configurations. Thus the magnetic field has the form $\mathbf{B} = \mathbf{B}_p + B_\phi \hat{\phi}$, with $\mathbf{B}_p = B_r \hat{r} + B_z \hat{z}$. We have $B_r = -(1/r)\partial\Psi/\partial z$ and $B_z = (1/r)\partial\Psi/\partial r$. where $\Psi(r, z) \equiv rA_\phi(r, z)$ is the flux function.

Most of the azimuthal twist $\Delta\phi$ of a field line of the Poynting jet occurs along the jet from $z = 0$ to $Z(t)$ as sketched in Figure 1a, where $Z(t)$ is the axial location of the ‘‘head’’ of the jet. Along most of the distance $z = 0$ to Z , the radius of the jet is a constant and $\Psi = \Psi(r)$ for $Z \gg r_0$, where r_0 is the radius of the O-point of the magnetic field in the disk. Note that the function $\Psi(r)$ is different from $\Psi(r, 0)$ which is the flux function profile on the disk surface. Hence $r^2 d\phi/dz = rB_\phi(r, z)/B_z(r, z)$. We take for simplicity $V_z = dZ/dt = \text{const.}$ We determine V_z subsequently. In this case $H(\Psi) = [r^2\Omega(\Psi)/V_z]B_z$ can be written as a function of Ψ and $d\Psi/dr$. With H known, the relativistic Grad-Shafranov equation,

$$\left[1 - \left(\frac{r\Omega}{c}\right)^2\right] \Delta^* \Psi - \frac{\nabla \Psi}{2r^2} \cdot \nabla \left(\frac{r^4 \Omega^2}{c^2}\right) = -H(\Psi) \frac{dH(\Psi)}{d\Psi}, \quad (1)$$

can be solved (Lovelace & Romanova 2003).

The quantity not determined by equation (1) is the velocity V_z , or Lorentz factor $\Gamma = 1/(1 - V_z^2/c^2)^{1/2}$. This is determined by taking into account the balance of axial forces at the head of the jet: the electromagnetic pressure within the jet is balanced against the dynamic pressure of the external medium which

is assumed uniform with density ρ_{ext} . This gives $(\Gamma^2 - 1)^3 = B_0^2/(8\pi\mathcal{R}^2\rho_{ext}c^2)$, or for $\Gamma \gg 1$,

$$\Gamma \approx 8 \left(\frac{10}{\mathcal{R}} \right)^{1/3} \left(\frac{B_0}{10^3 \text{G}} \right)^{1/3} \left(\frac{1/\text{cm}^3}{n_{ext}} \right)^{1/6}, \quad (2)$$

where $\mathcal{R} = r_0/r_g \gg 1$ and $r_g \equiv GM/c^2$, and B_0 the magnetic field strength at the center of the disk. A necessary condition for the validity of this equation is that the axial speed of the counter-propagating fast magnetosonic wave (in the lab frame) be larger than V_z so that the jet is effectively ‘subsonic.’ This value of Γ is of the order of the Lorentz factors of the expansion of parsec-scale extragalactic radio jets observed with very-long-baseline-interferometry (see, e.g., Zensus *et al.* 1998). This interpretation assumes that the radiating electrons (and/or positrons) are accelerated to high Lorentz factors ($\gamma \sim 10^3$) at the jet front and move with a bulk Lorentz factor Γ relative to the observer. The luminosity of the $+z$ Poynting jet is $\dot{E}_j = c \int_0^{r_0} r dr E_r B_\phi / 2 = c B_0^2 \mathcal{R}^{3/2} r_g^2 / 3 \sim 2.1 \times 10^{46} (B_0/10^3 \text{G})^2 (\mathcal{R}/10)^{3/2} (M/10^9 M_\odot)^2 \text{ erg/s}$, where M is the mass of the black hole.

For long time-scales, the Poynting jet is time-dependent due to the angular momentum it extracts from the inner disk ($r < r_0$) which in turn causes r_0 to decrease with time (Lovelace *et al.* 2002). This loss of angular momentum leads to a “global magnetic instability” and collapse of the inner disk (Lovelace *et al.* 1994, 1997, 2002) and a corresponding outburst of energy in the jets from the two sides of the disk. Such outbursts may explain the flares of active galactic nuclei blazar sources (Romanova & Lovelace 1997; Levinson 1998) and the one-time outbursts of gamma ray burst sources (Katz 1997).

3. RELATIVISTIC ELECTROMAGNETIC PIC SIMULATIONS

We performed relativistic, fully electromagnetic, particle-in-cell simulations of the formation of jets from an accretion disk initially threaded by a dipole-like magnetic field. This was done using the code XOOPIIC developed by Verboncoeur, Langdon, and Gladd (1995). Earlier, Gisler, Lovelace, and Norman (1989) studied jet formation for a monopole type field using the relativistic PIC code ISIS. The geometry of the initial configuration is shown in Figure 1b. The computational region is a cylindrical “can,” $r = 0 - R_m$ and $z = 0 - Z_m$, with outflow boundary conditions on the outer boundaries, and the potential and particle emission specified on the disk surface $r = 0 - R_m$, $z = 0$. Equal fluxes of electrons and positrons are emitted so that the net emission is effectively space-charge-limited. About 10^5 particles were used in the simulations reported here. The behavior of the lower half-space ($z < 0$) is expected to be a mirror image of the upper half-space.

Figure 2 shows the formation of a relativistic jet. The gray scale indicates the logarithm of the density of electrons or positrons with 20 levels between the lightest (10^{12}) and darkest ($4 \times 10^{15}/\text{m}^3$). The lines are poloidal magnetic field lines \mathbf{B}_p . The total \mathbf{B} -field is shown in Figure 3. The computational region

has $(R_m, Z_m) = (50, 100)$ m, the initial \mathbf{B} -field is dipole-like with $B_z(0, 0) \equiv B_0 = 28.3$ G and an O-point at $(r, z) = (10, 0)$ m, and the electric potential at the center of the disk is $\Phi_0 = -10^7$ V relative to the outer region of the disk. Initially, the computational region was filled with a distribution of equal densities of electrons and positrons with $n_{\pm}(0, 0) = 3 \times 10^{13}/\text{m}^3$. Electrons and positrons are emitted with equal currents $I_{\pm} = 3 \times 10^5$ A from both the inner and the outer portions of the disk as indicated in Figure 1b with an axial speed much less than c . For a Keplerian disk with $r_0 \gg r_g$, the scalings are $\Phi_0 \sim B_0(r_0 r_g)^{1/2}$, $I \sim c B_0 r_0$ and the jet power is $\sim c B_0^2 r_0^{3/2} r_g^{1/2}$. The calculations were done on a 64×128 grid stretched in both the r and z directions so as to give much higher spatial resolution at small r and small z . These simulations show the formation of a quasi-stationary, collimated current-carrying jet. The Poynting flux power of the jet is $\dot{E}_j \approx 7 \times 10^{11}$ W and the particle kinetic energy power is $\approx 4.7 \times 10^{10}$ W. The charge density of the electron flow is partially neutralized by the positron flow. Simulations are planned with the positrons replaced by ions. Scaled Z-pinch experiments configured as shown in Figure 1b can allow further study of astrophysical jet formation.

We thank C. Birdsall, S. Colgate, H. Li, J. Verboncoeur, I. Wasserman, J. Wick, and T. Womack for valuable assistance and discussions. This work was supported in part by NASA grants NAG5-13060 and NAG5-13220, by NSF grant AST-0307817, and by DOE cooperative agreement DE-FC03 02NA00057.

REFERENCES

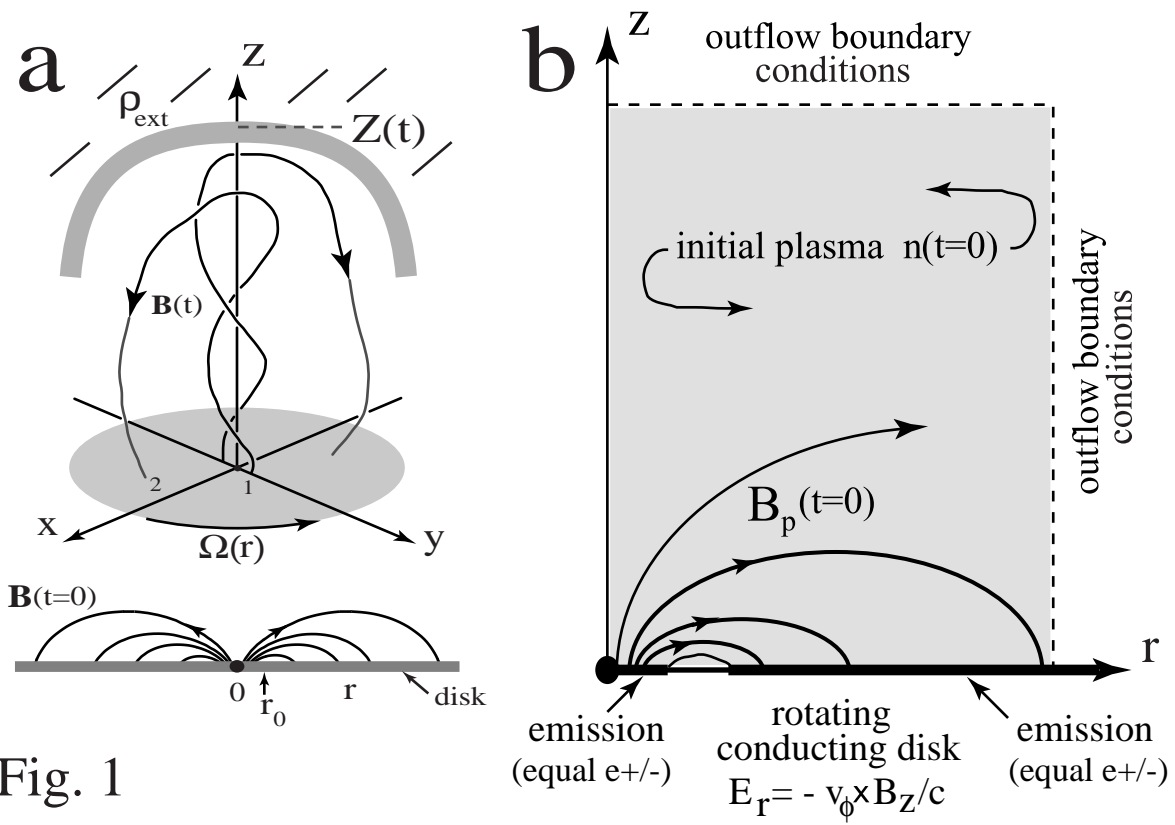
- Bisnovatyi-Kogan, G.S. & Lovelace, R.V.E. 2001, *New Astron. Rev.*, 45, 663
- Bridle, A.H., & Eilek, J.A. (eds.) 1984, in *Physics of Energy Transport in Extragalactic Radio Sources*, (Greenbank:- NRAO)
- Bührke, T., Mundt, R., & Ray, T.P. 1988, *A&A*, 200, 99
- Eikenberry, S., Matthews, K., Morgan, E.H., Remillard, R.A., & Nelson, R.W. 1998, *ApJ*, 494, L61
- Gisler, G., Lovelace, R.V.E., & Norman, M.L. 1989, *ApJ*, 342, 135
- Gold, T., & Hoyle, F. 1960, *MNRAS*, 120, 89
- Katz, J.I. 1997, *ApJ*, 490, 633
- Levinson, A. 1998, *ApJ*, S07, 145
- Li, H., Lovelace, R.V.E., Finn, J.M., & Colgate, S.A. 2001, *ApJ*, 561, 915
- Lovelace, R.V.E., Li, H., Koldoba, A.V., Ustyugova, G.V., & Romanova, M.M. 2002, *ApJ*, 572, 445
- Lovelace, R.V.E., Newman, W.I., & Romanova, M.M. 1997, *ApJ*, 484, 628
- Lovelace, R.V.E., Romanova, M.M., & Newman, W.I. 1994, *ApJ*, 437, 136
- Lovelace, R.V.E., Wang, J.C.L., & Sulkanen, M.E. 1987, *ApJ*, 315, 504
- Lovelace, R.V.E., & Romanova, M.M. 2003, *ApJ*, 596, L159
- Lynden-Bell, D. 1996, *MNRAS*, 279, 389

Figure 1: **(a)** Sketch of the magnetic field configuration of a Poynting jet from Lovelace and Romanova (2003). The bottom part of **(a)** shows the initial dipole-like magnetic field threading the disk which rotates at the angular rate $\Omega(r)$. The top part shows the jet at some time later when the head of the jet is at a distance $Z(t)$. At the head of the jet there is force balance between electromagnetic stress of the jet and the ram pressure of the ambient medium of density ρ_{ext} . **(b)** Sketch of the initial conditions for the relativistic PIC simulations of jet formation from an accretion disk.

- Mirabel, I.F., & Rodriguez, L.F. 1994 Nature, 371, 46
Romanova M.M., & Lovelace R.V.E. 1997, ApJ, 475, 97
Romanova, M.M., Ustyugova, G.V, Koldoba, A.V, Chechetkin, VM., & Lovelace, R.V.E. 1998, ApJ, 500, 703
Ustyugova, G.V, Lovelace, R.V.E., Romanova, M.M., Li, H., & Colgate, S.A. 2000 ApJ, 541, L21
Verboncoeur, J.P., Langdon, A.B., & Gladd, N.T. 1995, Comp. Phys. Comm., 87, 199
Zensus, J.A., Taylor, G.B., & Wrobel, J.M. (eds.) 1998, Radio Emission from Galactic and Extragalactic Compact Sources, IAU Colloquium 164, (Ast. Soc. of the Pacific)

Figure 2: Relativistic PIC simulations of the formation of a jet from a rotating disk. (a) -(c) give snapshots at times $(1, 2, 3) \times 10^{-7}$ s, and (d) is at $t = 10^{-6}$ s.

Figure 3: Three dimensional magnetic field lines originating from the disk at $r = 1, 2$ m for the same case as Figure 2.



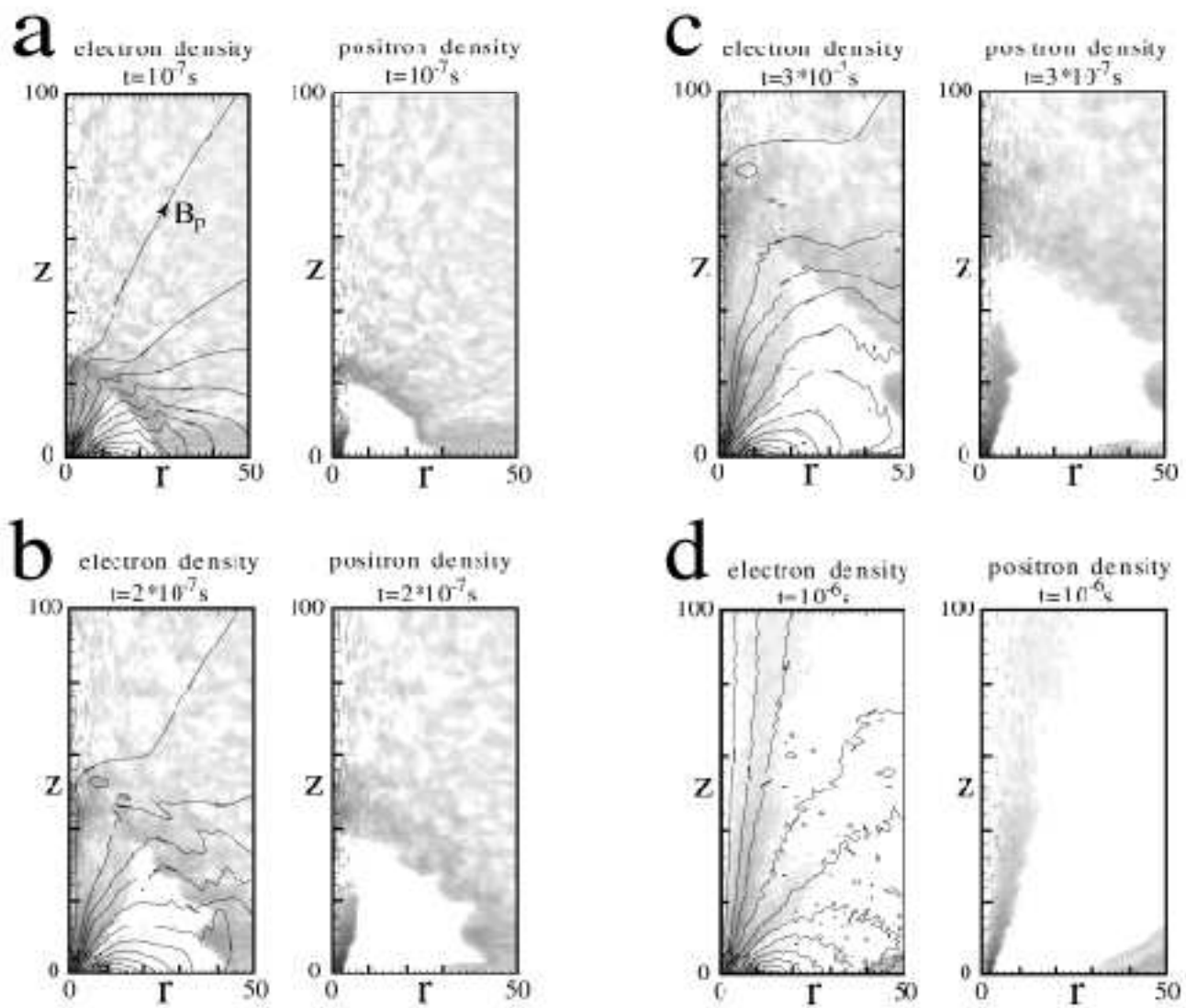


Fig. 2

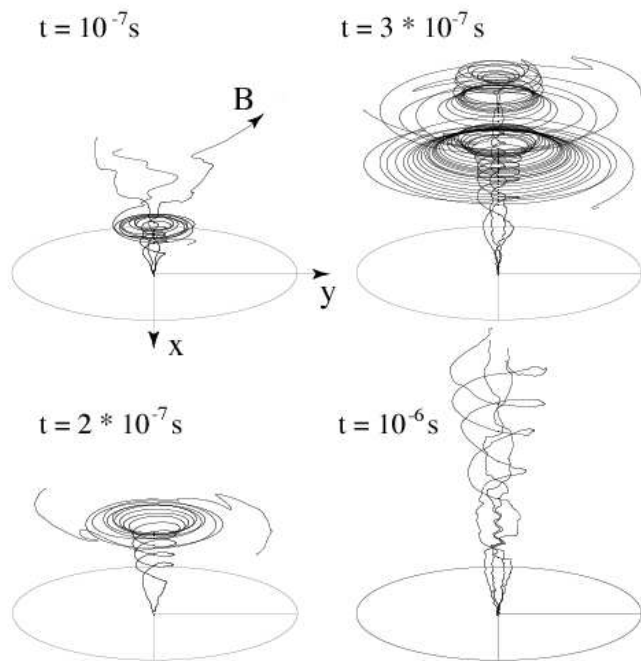


Fig. 3